Appl Phys B (2009) 96: 275–279
DOI 10.1007/s00340-009-3564-2

Applied Physics B
Lasers and Optics

Towards surface quantum optics with Bose–Einstein condensates in evanescent waves

H. Bender · P. Courteille · C. Zimmermann · S. Slama

Received: 21 January 2009 / Revised version: 1 April 2009 / Published online: 15 May 2009

Abstract We present a surface trap which enables the study of coherent interactions between ultracold atoms and evanescent waves. The trap combines a magnetic Joffe trap with a repulsive evanescent dipole potential. Exploiting the advantages of both approaches this technique improves recent surfaces traps, which are based either on magnetic or optical traps alone. On the one hand, the position of the magnetic trap can be controlled with high precision which makes it possible to move ultracold atoms to the surface of a glass prism or to withdraw the atoms from the surface in a controlled way. On the other hand, the optical potential of the evanescent wave partially compensates for strong attractive surface forces and generates a potential barrier at only a few hundred nanometers from the surface. This barrier prevents the surface potentials from limiting the trap depth of the magnetic trap. The surface trap is probed with ^{87}Rb Bose–Einstein condensates (BECs), which are stably positioned at distances from the surfaces below one micrometer.

PACS 42.50.-p · 32.80.Qk · 03.75.-b · 34.35.+a

1 Introduction

The interaction of ultracold atoms with surfaces has attracted much attention in the past for various technological and fundamental reasons. By the use of repulsive evanescent waves (EWs) at a prism surface atom mirrors were constructed from which both atomic beams and cold atomic clouds were reflected [1, 2]. EWs were also used for generating steep surface traps in which two-dimensional Bose–Einstein condensates can be prepared [3]. Atom-surface interactions are also interesting for investigating fundamental aspects of quantum electrodynamics. Close to surfaces the electromagnetic vacuum fluctuations lead to the emergence of surface potentials like van der Waals or Casimir–Polder potentials. These potentials have been investigated with hot atomic beams [4], in vapor nanocells [5], in atomic mirrors [6], by quantum reflection [7–10], and in magnetic traps [11]. Interestingly these potentials couple to surface phonons, which at very short distances may lead to a considerable heating effect on the atoms [12].

Inspired by the first atom mirror experiments, proposals have been developed for nondestructive detection of atoms by evanescent waves with the perspective of QND measurements of atomic number fluctuations [13, 14]. The idea was that atoms interacting with an EW act as a refractive index medium and thereby shift the phase of the totally reflected light field. A measurement of this phase shift should therefore reveal the atom number. By choosing a large detuning of the light frequency from atomic resonances, the atomic cloud remains undisturbed by this measurement. This proposal is complementary to experiments with resonant light fields which allow to measure the atom number destructively [15]. In the situation considered in [13] atoms are released from a magneto-optic trap (MOT) and bounce off an atom mirror. A quantitative analysis revealed a very small phase shift which will be barely detectable. The main problems are the facts that (1) the density of atoms from the MOT is too low and (2) the interaction time during the reflection is very short which results in a high shot noise. Other problems with reflection experiments are random scattering due to surface roughness [16–18]. We are able to circumvent these problems by using BECs which have four orders of magnitude

H. Bender · P. Courteille · C. Zimmermann · S. Slama (✉)
Physikalisches Institut, Eberhard-Karls-Universität Tübingen,
Auf der Morgenstelle 14, 72076 Tübingen, Germany
e-mail: slama@pit.physik.uni-tuebingen.de

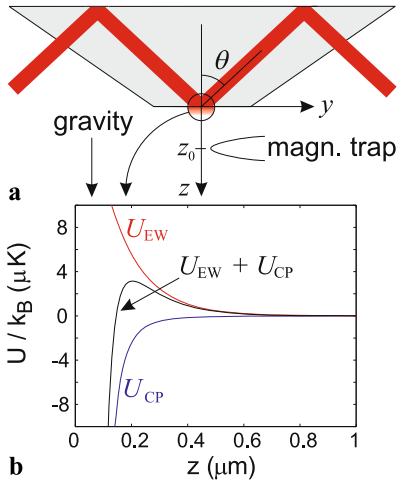

Fig. 1 (**a**) Schematic view of the prism. The magnetic trap is situated below the prism surface at a distance z_0 and can be shifted upward towards the surface, where the Casimir–Polder force and the repulsive dipole potential become dominant. This is illustrated in (**b**), where the Casimir–Polder potential U_{CP} and the evanescent wave potential U_{EW} add up to form a potential barrier at few hundred nanometers from the prism surface

larger densities and by keeping the atoms in a trap, which allows for adjusting the interaction time. Calculation with our parameters following the methods in [13] result in detectable phase shifts on the order of $\Delta\phi \sim 10^{-4}$ rad and signal-to-shot-noise ratios on the order of a few thousand.

The surface trap presented here uniquely combines the advantages of evanescent waves and magnetic fields. Magnetic traps have the advantage that they can be easily shifted by offset fields such that the atoms can be brought to the surface in a controlled way. However, magnetic traps are less steep than dipole traps. Therefore the problem occurs that the magnetic trapping potential is opened by the attractive Casimir–Polder potential close to surfaces which leads to the loss of atoms [19]. This can be avoided by an additional dipole potential that is generated by a blue detuned evanescent wave (Fig. 1a). The repulsive dipole potential is able to partially compensate for the Casimir–Polder potential thereby producing a potential barrier at only a few hundred nanometers from the surface (Fig. 1b). This potential barrier prevents the atoms from being lost when the magnetic trap is shifted to the surface.

2 Simulation of the surface trap

In the following, simulations of our combined surface trap are shown. The trapping potential is determined by the Casimir–Polder potential U_{CP}, the evanescent wave potential U_{EW}, the magnetic trapping potential U_{magn}, and the gravitational potential U_{g}

$$U_{\mathrm{tot}} = U_{\mathrm{CP}} + U_{\mathrm{EW}} + U_{\mathrm{magn}} + U_{\mathrm{g}}. \tag{1}$$

For the simulation of the surface potential, we use the formula for the retarded regime

$$U_{\mathrm{CP}}(z) = -\frac{C_4}{z^4}, \tag{2}$$

which at the distances relevant for our simulations is a sufficient approximation, although more precise interpolation formulas exist [9]. The variables in (2) are the distance from the surface z and the C_4 coefficient

$$C_4 = \frac{1}{4\pi\epsilon_0} \cdot \frac{3\hbar c\alpha(0)}{8\pi} \cdot \frac{\epsilon(0)-1}{\epsilon(0)+1} \cdot \Phi\big(\epsilon(0)\big), \tag{3}$$

where ϵ_0 is the dielectric permittivity of vacuum, c is the speed of light, $\alpha(0) = 5.26 \times 10^{-39}$ fm^2 the static polarizability of Rb, $\epsilon(0) = 2.25$ the static dielectric constant of the glass substrate corresponding to a refractive index of $n = 1.5$ and $\Phi(2.25) = 0.29$ is given by a formula in [20]. From these values we get a C_4 coefficient of $C_4 = 1.78 \times 10^{-55}$ J m^4. The evanescent wave potential exponentially decays with distance from the surface z and has a Gaussian shape in the transverse direction x, y with beamwaists $w_{x,y}$:

$$U_{\mathrm{EW}}(x,y,z) = U_0 \cdot \exp\left\{-2\frac{z}{\lambda_p} - 2\frac{x^2}{w_x^2} - 2\frac{y^2}{w_y^2}\right\}, \tag{4}$$

where the decay length is given by

$$\lambda_p = \left(k \cdot \sqrt{n^2 \sin(\theta)^2 - 1}\right)^{-1}, \tag{5}$$

with $k = 2\pi/\lambda$ the wavevector of the light with wavelength $\lambda = 765$ nm and θ the incidence angle (see Fig. 1). The maximum value of the potential at the surface is given by the dipole potential

$$U_0 = \frac{\pi c^2 \Gamma}{2\omega^3} \cdot \left(\frac{2}{\Delta_2} + \frac{1}{\Delta_1}\right) I_{\mathrm{ev}} \tag{6}$$

with $\Gamma = 2\pi \times 6$ MHz the natural linewidth of the Rb 5P state, ω the frequency of light, I_{ev} the maximum light intensity in the evanescent wave, and $\Delta_{1,2}$ the detuning of the laser frequency from the Rb D_1 and D_2 line. The magnetic trap is harmonic

$$U_{\mathrm{magn}}(x,y,z) = \frac{1}{2}m\left(\omega_x^2 x^2 + \omega_y^2 y^2 + \omega_z^2 (z-z_0)^2\right) \tag{7}$$

with trap frequencies of $\omega_x \sim 2\pi \times 25$ Hz, $\omega_y = \omega_z \sim 2\pi \times 200$ Hz, and m the atomic mass. The magnetic field minimum is located at a distance from the surface z_0 which is adjustable in our experiment. In good approximation the transverse coordinates of the magnetic field minimum coincide with the position of maximum evanescent light intensity. Finally the gravitational potential is given by

$$U_{\mathrm{g}}(z) = -mgz, \tag{8}$$

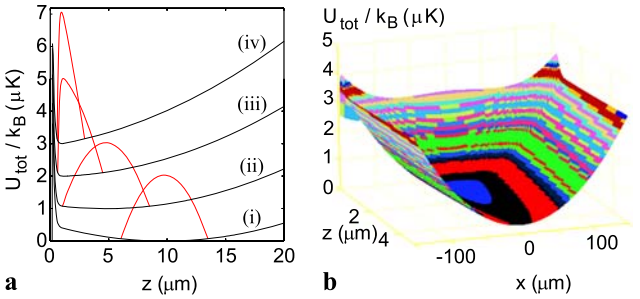

Fig. 2 (**a**) Simulated potential and atom density for different positions of the magnetic minimum z_0: (i) $z_0 = 0$ μm, (ii) $z_0 = -5$ μm, (iii) $z_0 = -10$ μm and (iv) $z_0 = -15$ μm. The curves are shifted relative to each other by 1 μK for better visibility. In these simulations the laser power is $P = 500$ mW, the reflection angle is $\theta = 47.5°$ corresponding to a decay length of $\lambda_p = 243$ nm, and the beamwaists are $w_x = 170$ μm and $w_y = 240$ μm. (**b**) Two-dimensional plot of the simulation result corresponding to curve (iv) in (**a**). The atomic density is omitted here for clarity

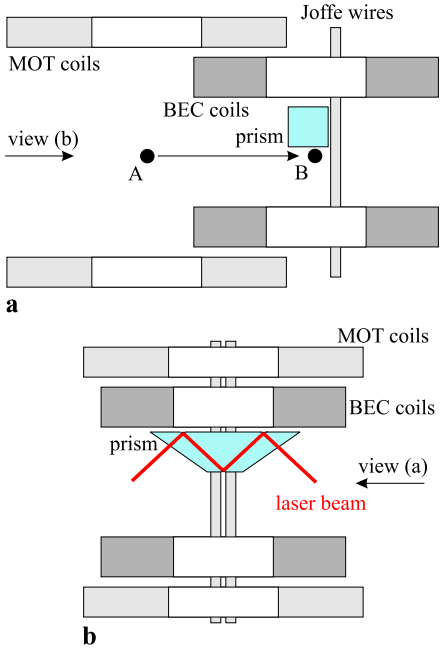

Fig. 3 (**a**, **b**) Schematic side views of the experimental setup. The magneto-optic trap is produced at position A. After adiabatic transfer to position B the atoms are evaporatively cooled in a Joffe–Pritchard type of wire trap, which is located about 100 μm below the surface of a glass prism. The Bose-condensed atoms are shifted in the magnetic trap to the surface. After the interaction they are withdrawn from the surface and then let adiabatically expanded for absorption imaging

where the negative sign accounts for the fact that the prism is mounted upside down in the chamber. The gravitational sag of the magnetic trap is 10 μm.

Figure 2a shows simulations of realistic trapping potentials for different positions of the magnetic field minimum z_0. Negative values of z_0 correspond to magnetic field minima behind the prism surface. The actual position of the trap though is at positive z values due to the combination with the other potentials, for example due to gravitational sagging. In addition, the atomic density in Thomas Fermi approximation is plotted for $N = 10^5$ atoms. By shifting the trap towards the surface the atomic cloud is compressed. Figure 2a shows a cut through the center of the trap along the z-axis. Figure 2b shows the simulated potential as a function of both z- and x-axes. A small reduction of the trap depth due to two saddle points is observed at about $x = \pm 70$ μm, because of the transversal Gaussian shape of the repulsive dipole potential.

3 Loading the surface trap with a ^{87}Rb BEC

The schematic setup of our experiment is sketched in Fig. 3. At position A ^{87}Rb atoms are collected in a magneto-optic trap. After loading into a purely magnetic trap the atoms are adiabatically transferred to a Joffe–Pritchard type of wire trap which is formed by a second pair of coils (BEC coils) and two wires which are running vertically through the coils. There the atoms are further cooled by forced evaporation. Within this trap we can produce Bose–Einstein condensates with up to approximately 6×10^5 atoms. The special feature of this wire trap is the fact that it can be easily shifted vertically by applying an external offset field. By this we are able to move the atoms very close to the surface of a glass prism which is mounted at the upper magnetic coil. The prism being attached upside down enables us to analyze the atomic cloud after the interaction with the prism surface in time-of-flight (TOF) absorption imaging.

The position of the trap $z_{\min}$ as a function of the position of the magnetic field minimum z_0 is illustrated in Fig. 4a. At distances of more than about one micrometer from the surface, the trap shifts with the magnetic field minimum. This is consistent with a linear fit of the simulated data points in regime (i) in Fig. 4a which shows a gradient of $\frac{dz_{\min}}{dz_0} = 1$. The offset of 10 μm is due to gravitational sagging. At distances to the surface of below about 1 μm the atoms cannot follow the magnetic potential any more but are held back by the evanescent wave potential barrier (regime [ii]). Only a small shift remains on the order of below $\frac{dz_{\min}}{dz_0} \sim 0.01$. The magnetic field at the position of the atoms B_A therefore increases. We have measured this increase with radio-frequency (RF) spectroscopy. For each position of the magnetic field minimum the radio frequency is detuned at which the atoms are resonantly coupled to an untrapped Zeeman state and thus lost from the trap. The transition frequency is given by the magnetic field B via $\hbar\omega_{\rm rf} = g_{\rm F}\Delta m_{\rm F}\mu_{\rm B}B$, with $g_{\rm F}$ the Landé factor, $\Delta m_{\rm F}$ the difference in the magnetic quantum number, and $\mu_{\rm B}$ the Bohr magneton. By determining the minimum radio frequency at which atom losses occur we get the magnetic field at the bottom of the trap. The

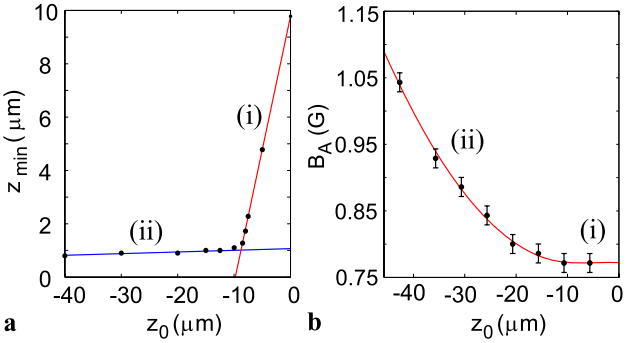

Fig. 4 (**a**) Simulated position of the trapping minimum $z_{\min}$ as a function of the position of the magnetic field minimum z_0. Negative values of z_0 correspond to a magnetic field minimum behind the prism surface. The simulated data points are fitted by two linear curves corresponding to the two regimes, where (i) the trap is moving along with the magnetic trap and (ii) the trap is held back by the potential barrier at the surface. (**b**) Measured magnetic field B_A at the position of the atoms as a function of z_0. In regime (i) B_A stays constant, whereas in regime (ii) B_A is rising quadratically. *Error bars* are due to the uncertainty in the measured radio frequency

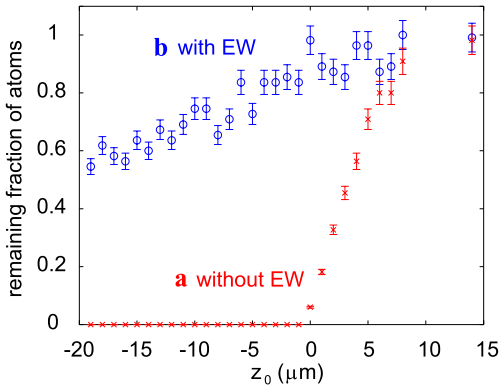

Fig. 5 Remaining fraction of atoms in the surface trap as a function of the magnetic field minimum z_0. We observe in curve (a) that without the potential barrier of the evanescent wave, all atoms are lost at a distance of approximately $z_{\min} = 10$ μm. With the evanescent wave (curve (b)) atom losses are strongly reduced such that the atoms can be positioned at distances from the surface below one micrometer. The *error bars* are due to an uncertainty in the measured atom number of 10%

result is shown in Fig. 4b. As we ramp the currents in the magnetic coils and thereby shift the magnetic trap towards the prism, we observe the transition from regime (i) where the magnetic offset field is constant to regime (ii) where it grows quadratically. A fit to the data reveals a magnetic trapping frequency of $\omega_z = 2\pi \times 195$ Hz, which is in good agreement with the value observed in trap oscillations. We have calibrated the relative shift of the magnetic field minimum to the currents in the magnetic coils by absorption imaging at larger distances from the surface. The absolute scale is fixed by the position where the magnetic offset field starts to rise quadratically. This position is taken from the simulation in Fig. 4a. As it turns out to be very robust against changes in the simulation parameters, we assume that the absolute position of the magnetic field minimum is calibrated to an error of approximately 1 μm.

With the help of the evanescent wave the atom losses occurring in magnetic traps close to surfaces are strongly reduced (Fig. 5) [19]. Here, a Bose–Einstein condensate is initially prepared in a magnetic trap at about $z_{\min} = 40$ μm below the prism surface. Then the magnetic trap is shifted in $\tau = 200$ ms towards the prism surface to a distance z_0 of the magnetic field minimum. In order to shift the atoms smoothly the corresponding coil currents are ramped with a sinusoidal time dependance $I = I_0 + \Delta I \cdot \sin(\pi t/\tau)^2$. After the magnetic trap is immediately shifted back to its starting position within 100 ms, the atoms are released and counted. The experimental results are shown in Fig. 5. Without the evanescent wave (curve a) the atoms are lost as soon as the Casimir–Polder potential opens up the magnetic trap. With the given magnetic trapping frequencies this occurs at a distance of the atoms from the surface of approximately 10 μm. The observed width of the decrease of atoms can be well explained by an energy spread given by the chemical potential of the BEC. However, with the evanescent dipole potential (curve b), the atoms can be shifted much closer to the surface. The position of the magnetic field minimum of several 10 μm behind the surface corresponds to a distance of the atoms from the surface of below 1 μm. At such small distances about half of the atoms are lost within the measuring time. This loss rate can be further reduced by increasing the laser intensity and thereby the potential barrier. We therefore attribute the atom loss to (1) the evaporation of atoms over the barrier and (2) tunneling of atoms through the barrier. This surface trap could therefore be used to probe tunneling of atoms through evanescent wave barriers.

4 Conclusion

We have described a surface trap which combines the flexibility of magnetic traps with the high gradients of evanescent dipole potentials. In such a trap atoms can be stably brought to the surface of transparent media with distances below 1 μm, which is the range of evanescent waves and surface potentials. This is the key for various experiments with cold atoms in which surface properties are investigated and exploited. Important examples are the probing of dispersive potentials due to the van der Waals and Casimir forces [21] but also the fascinating idea of investigating bound surface-atom states by laser-induced quantum adsorption [22, 23], which is the analogue to photoassociation of atoms. The crucial question herein is if atoms can be trapped in these highly excited bound states and if these traps can be tailored by a suitable structuring of the surface. In this context surface plasmon polaritons which can be used to locally enhance evanescent waves above surfaces are very promising [24].

Acknowledgements We acknowledge financial support by the EuroQUASAR program of the European Science Foundation and by Projektförderung für Nachwuchswissenschaftler der Universität Tübingen. We would like to thank Robin Kaiser and Andreas Günther for helpful discussions.

References

1. V.I. Balyikin, V.S. Lethokov, Yu.B. Ovchinnikov, A.I. Sidorov, JETP Lett. **45**, 353 (1987)
2. M.A. Kasevich, D.S. Weiss, S. Chu, Opt. Lett. **15**, 607 (1990)
3. D. Rychtarik, B. Engeser, H.-C. Nägerl, R. Grimm, Phys. Rev. Lett. **92**, 173003 (2004)
4. V. Sandoghdar, C.I. Sukenik, E.A. Hinds, S. Haroche, Phys. Rev. Lett. **68**, 3432 (1992)
5. M. Fichet, G. Dutier, A. Yarovitsky, P. Todorov, I. Hamdi, I. Maurin, S. Saltiel, D. Sarkisyan, M.-P. Gorza, D. Bloch, M. Ducloy, Europhys. Lett. **77**, 54001 (2007)
6. A. Landragin, J.-Y. Courtois, G. Labeyrie, N. Vansteenkiste, C.I. Westbrook, A. Aspect, Phys. Rev. Lett. **77**, 1464 (1996)
7. F. Shimizu, Phys. Rev. Lett. **86**, 987 (2001)
8. H. Friedrich, G. Jacoby, C.G. Meister, Phys. Rev. A **65**, 032902 (2002)
9. V. Druzhinina, M. DeKieviet, Phys. Rev. Lett. **91**, 193202 (2003)
10. T.A. Pasquini, Y. Shin, C. Sanner, M. Saba, A. Schirotzek, D.E. Pritchard, W. Ketterle, Phys. Rev. Lett. **93**, 223201 (2004)
11. J.M. Obrecht, R.J. Wild, M. Antezza, L.P. Pitaevskii, S. Stringari, E.A. Cornell, Phys. Rev. Lett. **98**, 063201 (2007)
12. C. Henkel, M. Wilkens, Europhys. Lett. **47**, 414 (1999)
13. A. Aspect, R. Kaiser, N. Vansteenkiste, P. Vignolo, C.I. Westbrook, Phys. Rev. A **52**, 4704 (1995)
14. J.-Y. Courtois, J.-M. Courty, S. Reynaud, Phys. Rev. A **52**, 1507 (1995)
15. R.A. Cornelussen, A.H. van Amerongen, B.T. Wolschrijn, R.J.C. Spreeuw, H.B. van Linden van den Heuvell, Eur. Phys. J. D **21**, 347–351 (2002)
16. C. Henkel, K. Mølmer, R. Kaiser, N. Vansteenkiste, C.I. Westbrook, A. Aspect, Phys. Rev. A **55**, 1160 (1997)
17. V. Savalli, D. Stevens, J. Estève, P.D. Featonby, V. Josse, N. Westbrook, C.I. Westbrook, A. Aspect, Phys. Rev. Lett. **88**, 250404 (2002)
18. H. Perrin, Y. Colombe, B. Mercier, V. Lorent, C. Henkel, J. Phys. B, At. Mol. Opt. Phys. **39**, 4649 (2006)
19. Y.J. Lin, I. Teper, C. Chin, V. Vuletic, Phys. Rev. Lett. **92**, 050404 (2004)
20. I. Dzyaloshinskii, E. Lifshitz, L. Pitaevskii, Adv. Phys. **10**, 165 (1961)
21. S. Kallush, B. Segev, R. Côté, Eur. Phys. J. D **35**, 3 (2005)
22. T. Passerat de Silans, B. Farias, M. Oriá, M. Chevrollier, Appl. Phys. B **82**, 367 (2006)
23. A.E. Avanasiev, P.N. Melentiev, V.I. Balykin, JETP Lett. **86**, 172 (2007)
24. M. Righini, A.S. Zelenina, C. Girard, R. Quidant, Nat. Phys. **3**, 477 (2007)